Bioorganic & Medicinal Chemistry Letters 21 (2011) 622–627

Contents lists available at ScienceDirect

Bioorganic & Medicinal Chemistry Letters

journal homepage: www.elsevier.com/locate/bmcl

Efficient synthesis of trisaccharide saponins and their tumor cell killing effects through oncotic necrosis

Jian Gao [a], Xia Li [b], Guofeng Gu [c], Bin Sun [c], Min Cui [b], Mei Ji [a], Hong-Xiang Lou [a,*]

[a] Department of Natural Product Chemistry, School of Pharmaceutical Sciences, Shandong University, 44 West Wenhua Road, Jinan 250012, PR China
[b] School of Oceanology, Shandong University, Weihai 264209, PR China
[c] National Glycoengineering Research Center, Shandong University, 44 West Wenhua Road, Jinan 250012, PR China

ARTICLE INFO

Article history:
Received 16 November 2010
Revised 7 December 2010
Accepted 8 December 2010
Available online 13 December 2010

Keywords:
Saponin
Indioside E
Trisaccharide analogues
Cytotoxicity
Oncosis

ABSTRACT

To investigate the relationship of cytotoxicity and saponins with varied aglycones, based on the structure of indioside E **1**, a natural derived anti-tumor active ingredient from Chinese medicinal plant *Solanum indicum* L., five novel saponins **2–6** bearing the same trisaccharide moiety together with **1** were efficiently synthesized via a transglycosylation strategy. MTT assay revealed the killing effects to tumor cells of the synthesized saponins are varied with the change of aglycones. Furthermore, time-lapse microscopy, LDH release, PI staining, and immunocytochemical investigations demonstrated that the cell death caused by neosaponin **2** was through oncotic necrosis involving plasma membrane perturbation and destruction of cytoskeleton.

Natural derived saponins from terrestrial plants or marine organisms display a wide spectrum of structural diversity and versatile biological activities, which include anti-inflammatory, antibacterial, antiparasitic, antifungal, and anti-tumor activities.[1–5] Their biological effects were correlated to both their sugar residues and aglycones.[6,7] To exemplify the structure-activity relationship study, solamargine and solasonine, which have same aglycone but different composition of sugar moiety, showed different tumor cell killing results while OSW-1 and some of its disaccharide analogues, which have same sugar moiety but variant aglycones showed comparable anticancer activity.[8–11]

Indioside E (**1**, Fig. 1), namely diosgenyl α-L-rhamnopyranosyl-(1→2)-[β-D-xylopyranosyl-(1→3)]-β-D-galactopyranoside, was extracted from a traditional Chinese medicinal plant *Solanum indicum* L. herb.[12] Preliminary biological test showed that **1** exhibits promising cytotoxic activity toward human hepatocellular carcinoma BEL-7402.[13] Attracted by its potent anti-tumor activity and the importance of sugar residues for saponins, we exploited here the practical and efficient synthesis of indoiside E and its novel analogues **2–6** by introducing different aglycones with the same trisaccharide into the structure (Fig. 1) for searching new saponins with pronounced anticancer activity. Furthermore, the cytotoxicity of all the synthesized saponins **1–6** was assayed and the oncotic necrosis mechanism of the potent active compound was also revealed in present study.

Compound **1** has been previously synthesized using six straightforward sequential reactions,[13] the target neosaponins were assembled here by an efficient transglycosylation strategy, using the trisaccharide donor directly transferred to different aglycones. As shown in Scheme 1, isopropyl 3-*O*-fluorenylmethoxycarbonyl-4,6-di-*O*-benzylidene-1-thio-β-D-galactopyranoside **7** was regioselectively prepared from commercially available isopropyl β-D-thiogalactopyranoside (IPTG) according to the published procedure in two steps.[14] Thereafter, standard glycosylation of galactopyranosyl acceptor **7** with 2,3,4-tri-*O*-acetyl-α-L-rhamnopyranosyl trichloroacetimidate **8** in anhydrous CH_2Cl_2 using trimethylsilyl trifluoromethanesulfonate (TMSOTf) as catalyst provided α-(1→2)-linked disaccharide **9**, followed by triethylamine (TEA) promoted removal of Fmoc group on 3-OH of galactose unit of **9**, furnished the disaccharide acceptor **10** in excellent yield of 84% for two steps. Subsequently, under the promotion of TMSOTf, coupling of disaccharide acceptor **10** with benzoyl-protected xylosyl imidate **11** afforded thiotrisaccharide **12** as a potent glycosylation donor in 67% yield. It is noteworthy that the xylosyl residue in **12** adopts a $^1C_4$ conformation instead of the typical $^4C_1$ form. This conformational assignment was deduced from the small coupling constants ($J_{1,2}$ = 3.0 Hz, $J_{2,3}$ = $J_{3,4}$ = 3.6 Hz) observed in ^{1}H NMR spectrum. The chemical shift of C-1 (δ 99.7 ppm) in ^{13}C

* Corresponding author. Tel.: +86 531 88382012; fax: +86 531 88382019.
E-mail address: louhongxiang@sdu.edu.cn (H.-X. Lou).

0960-894X/$ - see front matter © 2010 Elsevier Ltd. All rights reserved.
doi:10.1016/j.bmcl.2010.12.046

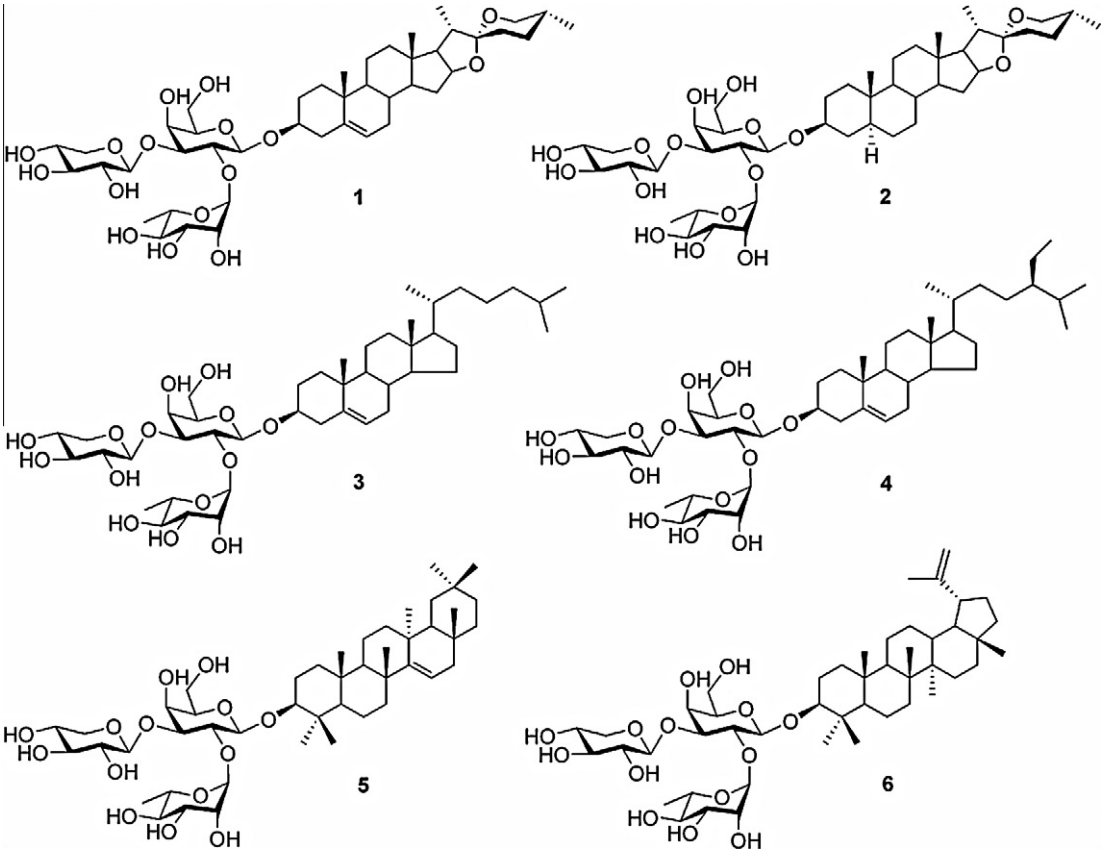

Figure 1. Structures of indioside E (**1**) and synthesized indioside E trisaccharide derivatives (**2**–**6**).

NMR spectrum confirmed the β-bond linkage between xylose and galactose residue in **12**.

Subsequently, thiotrisaccharide **12** was used as a glycosyl donor to transfer to aglycone by standard glycosylation. Unfortunately, direct glycosylation of diosgenin with **12** under the promotion of *N*-iodosuccinimide (NIS)-TMSOTf was troublesome. The reaction resulted in a complex mixture of products and the desired protected glycosides with poor yield and can only be detected by MS analysis. A detailed evaluation of the result suggested that thioglycoside **12** was not an active glycosyl donor matching 3-OH of diosgenin alycone in this glycosylation. To circumvent this problem, compound **6** was converted into more efficient trichloroacetimidate **14** in 81% yield for two steps as follows: (i) NIS and $HClO_4$ immobilized on silica (NIS/$HClO_4$-silica) promoted chemoselective hydrolysis of thioglycoside **12** in CH_2Cl_2–H_2O co-solvent system (→**13**);[15,16] (ii) trichloroacetimidate activation of anomeric carbon using trichloroacetonitrile (CCl_3CN) and 1,8-diazabicyclo[5.4.0]undec-7-ene (DBU) in dichloromethane. As expected, trisaccharide imidate **14** was successfully and efficiently transferred to the varied aglycones (e.g., diosgenin, tigogenin, cholesterol, sitosterol, taraxerol, and lupeol) in the presence of TMSOTf at 0 °C to afford the corresponding protected β-neoglycosides **15–20** in high yields of 81–87% as well as trace amount of their α isomers.[17] Interestingly, the stereo-selectivity of this glycosylation was predominantly β stereo-controlled without the neighboring group participation effect of donor **14**, which was adjusted by the coupling constants of the galactosyl H-1s ($J_{1,2}$ = ~7.8 Hz) in ^{1}H NMR spectra and the chemical shifts of C-1s (δ ~100.2 ppm). Global deprotection of pure β-protected glycosides **15–20** was accomplished in aqueous 80% acetic acid at 70 °C, followed by 1 N NaOH to furnish the target indoiside E **1** and noesaponins **2–6**.[18] The conformation of xylosyl residues in compounds **1–6** were converted back to $^4C_1$ form, supported by the doublet peaks of xylosyl H-1s at ~5.05 ppm ($J_{1,2}$ = ~7.8 Hz) in ^{1}H NMR spectra.

Table 1
The cytotoxicity of compounds **1**–**6** on four tumor cell lines

Compound	IC_{50} (μM)			
	K562	KB	MCF-7	U87
1	3.74	1.71	1.82	2.48
2	3.77	1.32	2.61	3.12
3	11.35	16.28	9.48	16.48
4	>40	>40	>40	>40
5	>40	>40	>40	>40
6	>40	>40	>40	>40

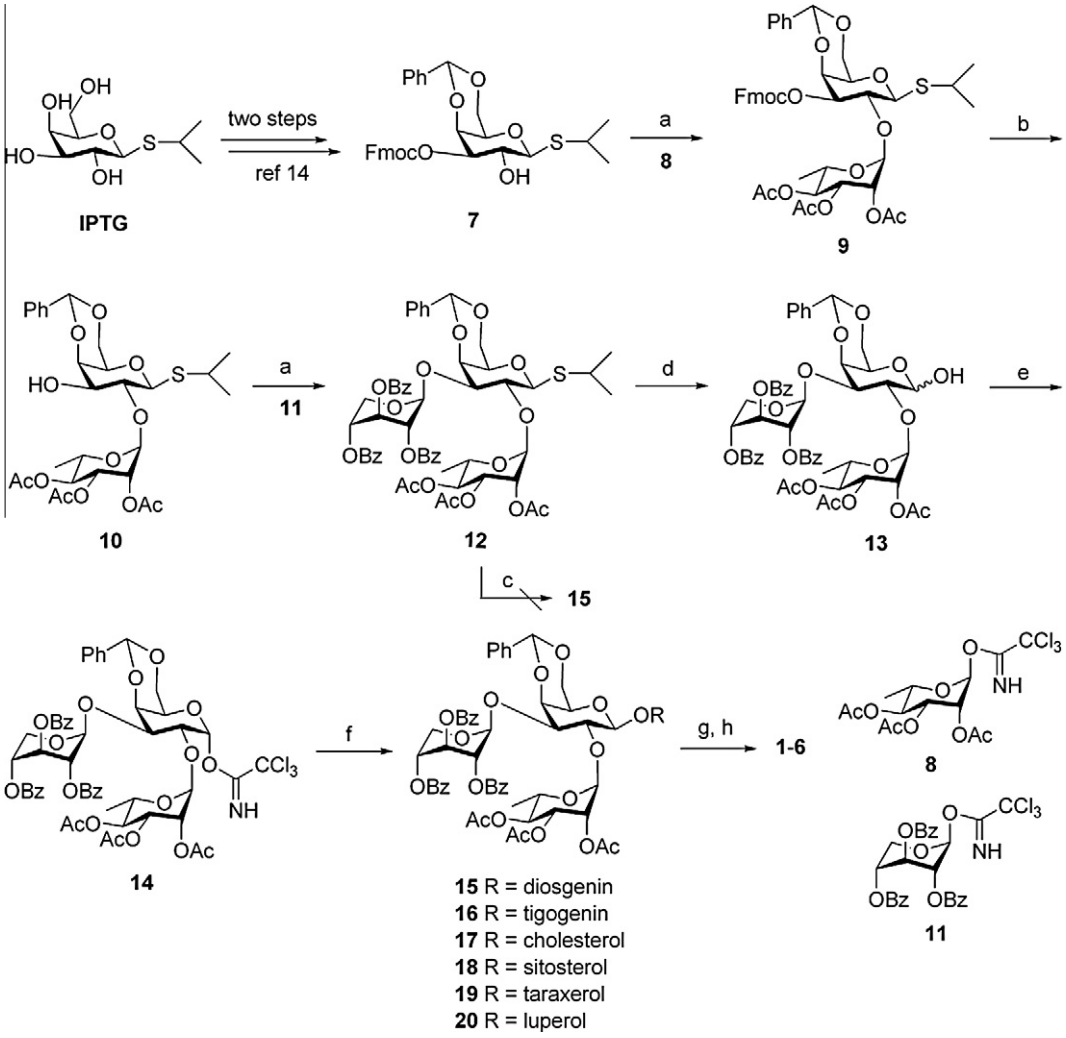

Scheme 1. Reagents and conditions: (a) TMSOTf, CH_2Cl_2, 0 °C, 45 min, 92% for **9**, 67% for **12**; (b) Et_3N, rt, 91%; (c) diosgenin, NIS-TMSOTf, −40 °C to rt; (d) NIS-$HClO_4/SiO_2$, CH_2Cl_2/H_2O 10:1, 0 °C, 1.5 h; (e) CCl_3CN, DBU, CH_2Cl_2, 0 °C, 2 h, 81% from **12**; (f) aglycones, TMSOTf, CH_2Cl_2, 0 °C, 40 min: diosgenin for **15**, 87%; tigogenin for **16**, 81%; cholesterol for **17**, 85%; sitosterol for **18**, 82%; taraxerol for **19**, 82%; lupeol for **20**, 87%; (g) aqueous 80% AcOH, 70 °C, 3 h; (h) 1 N CH_3ONa, CH_3OH/CH_2Cl_2 2:1, 3 h.

The cell killing effects of above synthesized saponins **1–6** on K562, KB, MCF-7 and U87 cells and three normal cell lines (HL7702, H9C2, and EVC304) was assayed using MTT method. As shown in Tables 1 and 2, both **1** and **2** displayed strong cell killing effects with IC_{50} ranging from 1.32 to 3.77 μM, but **2** had a lower cytotoxicity to normal hepatocyte cell HL7702. Compound **3** exhibited a moderate anti-tumor activity despite it is not so toxic to normal cells. Meanwhile, neosaponins **4–6** were inactive at a concentration of 40 μM. The results indicated that the spirostane-type aglycone part of **1** was of importance for its activity and taraxerol, lupeol, and sitosterol replacement will decrease the cytotoxicity.

The excellent anticancer activity and lower toxicity to HL7702 of neosaponin **2** encouraged us to investigate the possible mechanism of its action at the molecular level. Inspection of **2**-treated cells by means of time-lapse microscopy revealed the presence of cells swell and membrane surface blebs. Figure 2 showed that the blebs of K562 and MCF-7 formed as early as 30–60 min post-treatment with **2** and blebs last 15–30 min in these two cells. However, the cell swell last longer time and membrane disrupt at the end. The above results

Table 2
Cytotoxicity of **1–3** on normal cell lines

Compound	IC_{50} (μM)		
	EVC304	HL7702	H9C2
1	3.93	4.81	>20
2	4.03	6.92	>20
3	>20	>20	>20

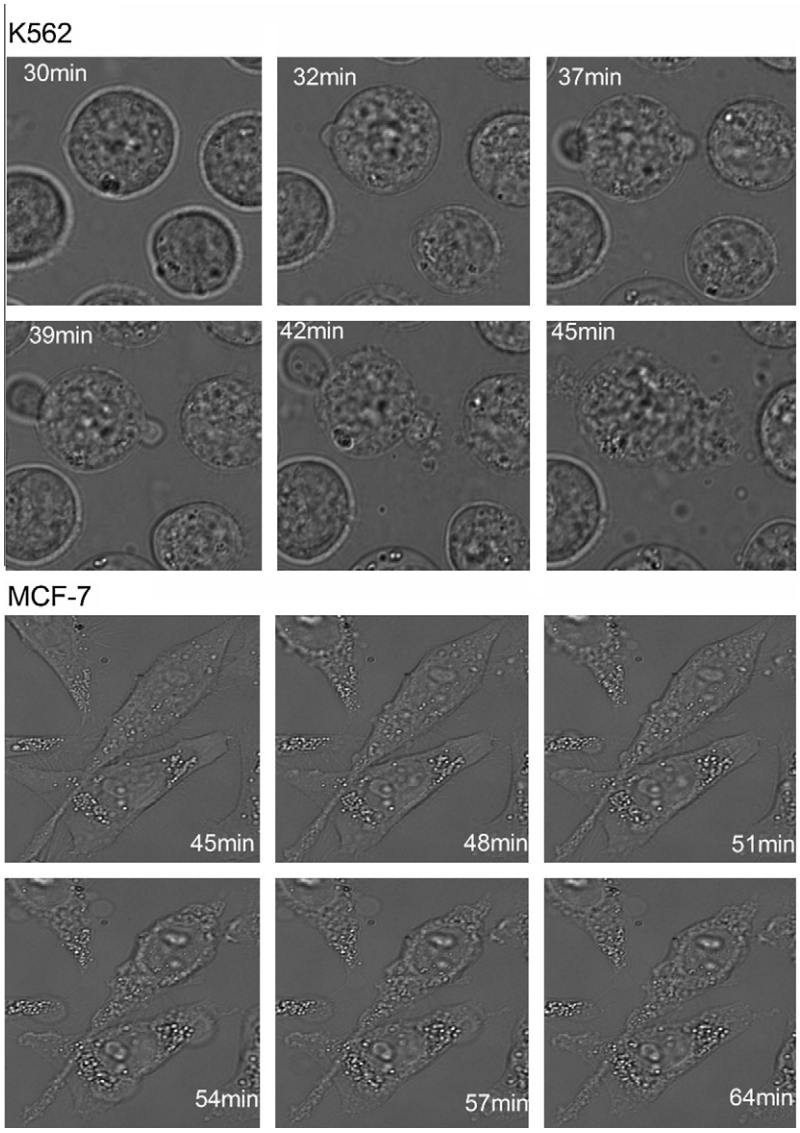

Figure 2. Time-lapse analysis of cell morphological changes and membrane blebs formation induced by 5 μM **2** in K562 and MCF-7 cells.

indicated compound **2** exhibited morphologic oncotic feature and resulted the damage of plasma membrane.

Plasma membrane integrity was monitored by measuring the release of the lactose dehydrogenase (LDH) into the incubation medium. The data showed that LDH release of K562 and MCF-7 cells were increased after 10 min treatment of 5 μM compound **2** and peaked at about 180 min (Fig. 3A).

The integrity of the cell membrane was also determined by the uptake of the PI (DNA intercalating fluorescent dye).[19] Staining of the cells with PI and subsequently analyzed by fluorescence microscopy. As shown in Figure 3B, the control cells unstained by PI and the cells treated with compound **2** stained by PI since the cell membrane was disrupted.

Several studies have suggested that surface bleb formation is related to alteration in cytoskeleton network.[20,21] Here, immunocytochemical investigations revealed the change of cytoskeleton network in compound **2**-exposed cells. As shown in Figure 4, the loss of microtubules and actins microfilaments were observed in **2**-treated cells. The results demonstrated that **2** induced plasma membrane blebs, which was related to its destroying microtubules and actins in culture cells.

The conformations of **1** and **2** were energy-minimized and superimposed, and the results are shown in Figure 5.[22] Obviously, there is a striking overlap of the calculated structures of **1** and **2** except for a few minor differences in their aglycones owing to the double bond of **1**. In consideration of the promising anticancer activity and lower toxicity to HL7702 of **2**, we can infer that the double bond of **1** may be a good active spot to modify in our next work.

In summary, indioside E **1** together with its five neosaponins **2-6** bearing the same trisaccharide residue were synthesized via an efficient transglycosylation strategy. A preliminary SAR analysis indicated that the spirotane-type aglycones of **1** and **2** are of value for their anticancer activity, and replacing diosgenin with tigogenin decrease cytotoxicity toward HL7702 without loss of anti-tumor activity. Furthermore, **2**-induced oncosis in K562 and MCF-7 cells is associated with both plasma membrane permeability and the disruption of cytoskeleton network. Collectively, our study suggest that **2** exhibits potent anti-tumor activity via a novel form of oncosis-like cell death and may merit further investigation as a potential therapeutic agent for cancer treatment. Much more work about the biochemical mechanism by which **2**-induced oncosis is required and is ongoing.

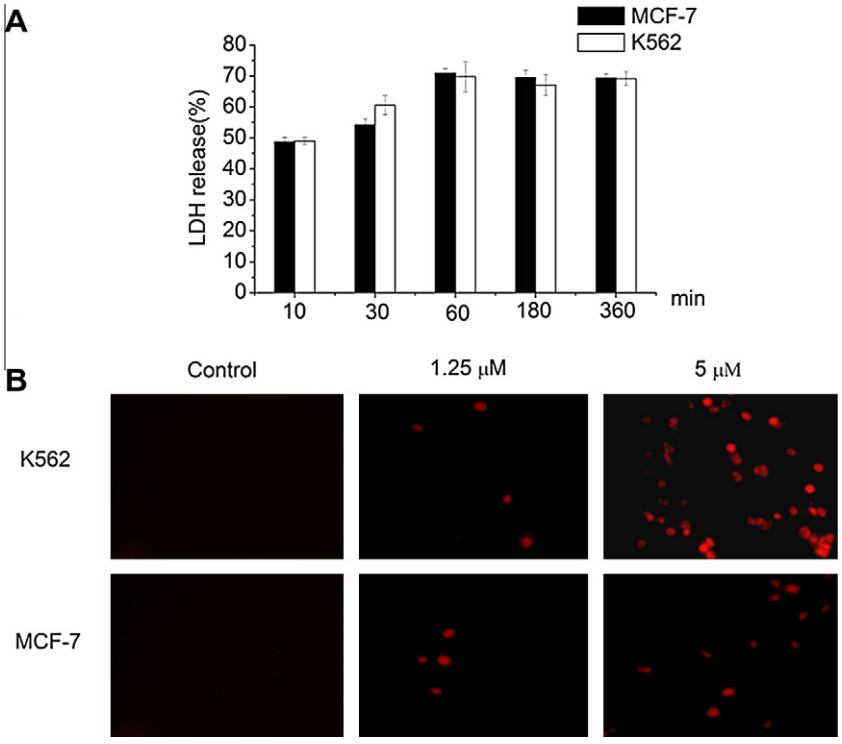

Figure 3. (A) **2**-induced LDH release from K562 and MCF-7cells. (B) PI uptake of K562 and KB cells after **2** treatment.

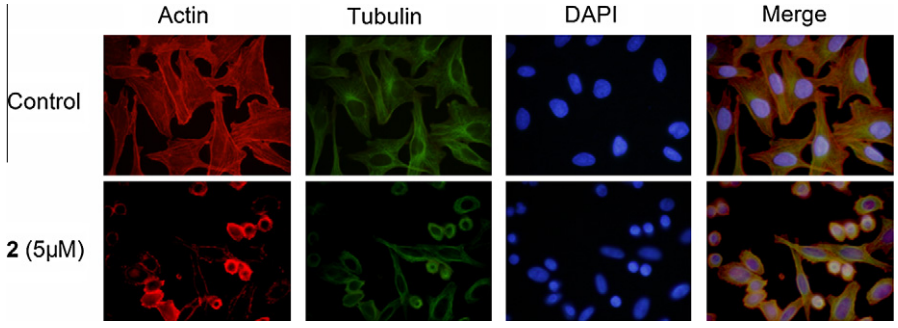

Figure 4. Effect of **2** on the microtubule and actin distribution in MCF-7 cells analyzed by a fluorescent microscope at magnification of 1000×.

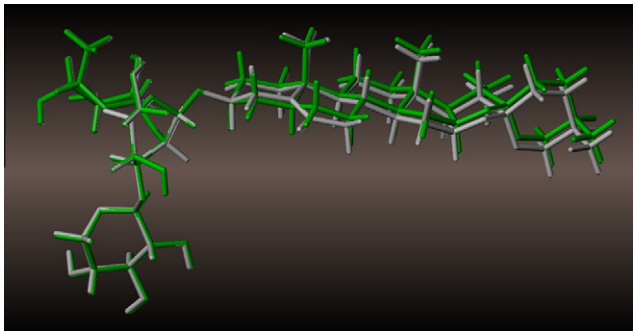

Figure 5. Three dimensional superimposition of the minimum energy structures: **1** (gray) and **2** (green).

Acknowledgments

This work was supported by grants from Shandong Provincial Foundation (Nos. 06GG1102023 and ZR2010BQ004).

Supplementary data

Supplementary data associated with this article can be found, in the online version, at doi:10.1016/j.bmcl.2010.12.046.

References and notes

1. Sparg, S. G.; Light, M. E.; van Staden, J. *J. Ethnopharmacol.* **2004**, *94*, 219.
2. Kwak, W. J.; Han, C. K.; Chang, H. W.; Kim, H. P.; Kang, S. S.; Son, K. H. *Chem. Pharm. Bull.* **2003**, *51*, 333.
3. Iorizzi, M.; Lanzotti, V.; Ranalli, G.; De Marino, S.; Zollo, F. *J. Agric. Food Chem.* **2002**, *50*, 4310.
4. De Lucca, A. J.; Bland, J. M.; Vigo, C. B.; Cushion, M.; Selitrennikoff, C. P.; Peter, J.; Walsh, T. *J. Med. Mycol.* **2002**, *40*, 131.
5. Tran, Q. L.; Tezuka, Y.; Banskota, A. H.; Tran, Q. K.; Saiki, I.; Kadota, S. *J. Nat. Prod.* **2001**, *64*, 1127.
6. Wang, Y.; Zhang, Y.; Zhu, Z.; Zhu, S.; Li, Y.; Li, M.; Yu, B. *Bioorg. Med. Chem.* **2007**, *15*, 2528.
7. Man, S.; Gao, W.; Zhang, Y.; Huang, L.; Liu, C. *Fitoterapia* **2010**, *81*, 703.
8. Liang, C. H.; Liu, L. F.; Shiu, L. Y.; Huang, Y. S.; Chang, L. C.; Kuo, K. W. *Biochem. Biophys. Res. Commun.* **2004**, *322*, 751.
9. Chang, L. C.; Tsai, T. R.; Wang, J. J.; Lin, C. N.; Kuo, K. W. *Biochem. Biophys. Res. Commun.* **1998**, *242*, 21.
10. Peng, W.; Tang, P.; Hu, X.; Liu, J. O.; Yu, B. *Bioorg. Med. Chem. Lett.* **2007**, *17*, 5506.

11. Zheng, D.; Zhou, L.; Guan, Y.; Chen, X.; Zhou, W.; Chen, X.; Lei, P. *Bioorg. Med. Chem. Lett.* **2010**, *20*, 5439.
12. Yahara, S.; Nakamura, T.; Someya, Y.; Matsumoto, T.; Yamashita, T.; Nohara, T. *Phytochemistry* **1996**, *43*, 1319.
13. Gu, G.; Du, Y.; Linhardt, R. J. *J. Org. Chem.* **2004**, *69*, 5497.
14. Roussel, F.; Knerr, L.; Grathwohl, M.; Schmidt, R. R. *Org. Lett.* **2000**, *2*, 3043.
15. Dasgupta, S.; Roy, B.; Mukhopadhyay, B. *Carbohydr. Res.* **2006**, *341*, 2708.
16. Du, Y.; Wei, G.; Cheng, S.; Hua, Y.; Linhardt, R. J. *Tetrahedron Lett.* **2006**, *47*, 307.
17. *General procedure for preparation of compounds* **15**–**20**: The mixture of each aglycone (0.13 mmol, diosgenin, tigogenin, cholesterol, sitosterol, taraxerol, or lupeol.) and trichloroacetimidate **14** (100 mg, 0.089 mmol) was dissolved in anhydrous CH_2Cl_2 (4 mL). To the solution was added TMSOTf (1.6 μL, 9 μmol) at 0 °C under N_2 protection. The reaction mixture was stirred for 40 min, neutralized with Et_3N, concentrated under reduced pressure. The residue was subjected to flash column chromatography (SiO_2) with a 5:1 solution of petroleum ether–EtOAc to afford the protected glycosides **15**–**20** in the form of β isomer with the yield ranging from 81% to 87%.
18. Physical and analytical data for neosaponin tigogenyl 3-*O*-{α-L-rhamnopyranosyl-(1→2)-[β-D-xylopyranosyl-(1→3)]-β-D-galactopyranoside} (**2**). $[\alpha]_D^{20}$ −96 (*c* 0.3, pyridine). Selected ^{1}H NMR (600 MHz, pyridine-d_5) δ 0.69 (d, *J* = 5.4 Hz, 1H), 0.82, 0.87 (2s, 2 × 3H), 1.14 (d, *J* = 7.2 Hz, 3H), 1.68 (d, *J* = 6.0 Hz, 3H, rha H-6), 3.49–3.67 (m, 3H), 3.92 (t, *J* = 8.1 Hz, 1H), 4.01–4.05 (m, 1H), 4.09–4.19 (m, 3H), 4.23–4.26 (m, 2H), 4.30 (t, *J* = 9.6 Hz, 1H), 4.42–4.49 (m, 2H), 4.54 (q, *J* = 7.8 Hz, 1H), 4.61 (dd, *J* = 3.0, 9.0 Hz, 1H), 4.70 (t, *J* = 7.8 Hz, 1H), 4.80 (d, *J* = 2.4 Hz, 1H), 4.87–4.90 (m, 1H), 4.92 (d, *J* = 6.0 Hz, 1H), 5.02 (d, *J* = 7.8 Hz, 1H, gal H-1), 5.06 (d, *J* = 7.8 Hz, 1H, xyl H-1), 6.27 (s, 1H, rha H-1). ^{13}C NMR (150 MHz, pyridine-d_5) δ 15.4, 16.9, 17.7, 19.0, 19.7, 21.6, 29.3, 29.6, 30.2, 30.9, 32.1, 32.5, 32.7, 34.5, 35.6, 36.2, 37.5, 40.4, 41.1, 42.3, 44.8, 54.7, 56.7, 62.7, 63.3, 67.1, 67.4, 69.7, 70.8, 71.4, 72.9, 73.2, 74.4, 75.1, 75.7, 76.7, 76.9, 78.7, 81.4, 85.4, 100.2 (gal C-1), 102.6 (rha C-1), 107.2 (xyl C-1), 109.5. HR-ESI-MS *m*/*z* calcd for $C_{44}H_{72}O_{16}Na$ ($M+Na^+$): 879.4713; found 879.4719.
19. Wang, K. R.; Yan, J. X.; Zhang, B. Z.; Song, J. J.; Jia, P. F.; Wang, R. *Cancer Lett.* **2009**, *278*, 65.
20. Neisch, A. L.; Speck, O.; Stronach, B.; Fehon, R. G. *J. Cell Biol.* **2010**, *189*, 311.
21. Malorni, W.; Iosi, F.; Mirabelli, F.; Bellomo, G. *Chem. Biol. Interact.* **1991**, *80*, 217.
22. Superimposition was calculated by Molecular Modeling System SYBYL-X-1.1; Tripos Associates, Inc.